3P6-3

Effect of Signal Retransmission Interval on Communication Quality in Underwater Acoustic Communication Using Time-diversity and Orthogonal Signal Division Multiplexing

Junnosuke Yoshita[‡], Tadashi Ebihara[*], Naoto Wakatsuki, and Yuka Maeda (Univ. Tsukuba)

1. Introduction

Underwater acoustic (UWA) communication is an essential foundational technology for the efficient operation of underwater vehicles. However, UWA channels have significant delay and Doppler spreads compared to radio channels [1], and numerous studies have been conducted to overcome these issues including array processing[2-4]. For example, the use of a multichannel receiver (Rx) has been found to effectively improve communication quality, when the UWA channels from the emitter at the transmitter (Tx) to each hydrophone at the Rx are independent. However, this results in an Rx with a large architecture, which becomes a barrier for underwater vehicles with limited capacity.

Therefore, this study focuses on UWA communication using time-diversity. Time-diversity improves communication quality with a single channel receiver; the Tx emits the signal multiple times to dynamic channel at different time intervals, and the Rx combines signals that have passed through independent channels. However, the relationship between communication quality and the intervals has not been well clarified. Therefore, in this paper, we investigated the performance of UWA communication using time-diversity and orthogonal signal division multiplexing (OSDM) by varying the parameter.

2. Overview of UWA communication using time-diversity and OSDM

Figure 1 shows an overview of UWA communication using time-diversity and OSDM. As shown in the figure, we assume that the Tx and Rx are set on a mobile and fixed platform, respectively.

The Tx reads a pilot signal $\boldsymbol{p}$ and message $\boldsymbol{m}$, performs OSDM modulation (output: $\boldsymbol{x}$), up-converts the modulated signal, and emits the signal through the UWA channel multiple times β at specific intervals δ.

Note that the OSDM signal $\boldsymbol{x}$ can be represented as

$$\boldsymbol{x} = \left(\boldsymbol{p}, \boldsymbol{0}_{1\times 2QM}, \boldsymbol{x}, \boldsymbol{0}_{1\times 2QM}\right)\left(\boldsymbol{F}_N \otimes \boldsymbol{I}_M\right), \quad (1)$$

where $\boldsymbol{p}$ and $\boldsymbol{x}$ are vectors of size $1\times M$, whose element is a complex symbol, $\boldsymbol{0}_{1\times 2QM}$ is a zeros matrix of size $1\times 2QM$, $\boldsymbol{F}_N$ is an inverse discrete Fourier transform matrix of size $N\times N$ ($N = 4Q+2$

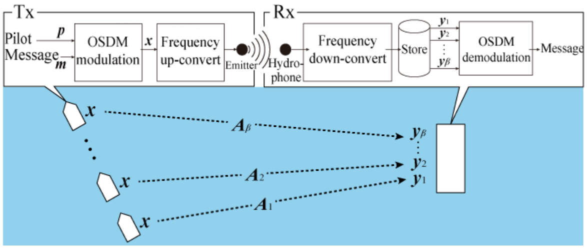

Fig. 1 Block diagram of UWA communication using time-diversity and OSDM.

and Q is the maximum Doppler shift), and $\boldsymbol{I}_M$ is an identity matrix of size $M\times M$, respectively.

The Rx receives the signal with a hydrophone, down-converts it (output: $\boldsymbol{y}_k$, $k = 1, 2, \ldots, \beta$), stores the signal, and performs OSDM demodulation by combining $\boldsymbol{y}_k$.

Specifically, the received signal $\boldsymbol{y}_k$ can be represented as

$$\boldsymbol{y}_k = \boldsymbol{x}\boldsymbol{A}_k + \boldsymbol{\eta}_k = \boldsymbol{x}\sum_{q=-Q}^{Q} \boldsymbol{H}_{k,q}\boldsymbol{\Lambda}_q + \boldsymbol{\eta}_k, (2)$$

where $\boldsymbol{y}_k$, $\boldsymbol{H}_{k,q}$, Λ_q, and $\boldsymbol{\eta}_k$ are a vector of size $1\times MN$, a channel matrix of size $MN\times MN$ corresponding to Doppler shift q, a diagonal matrix of size $MN\times MN$ representing Doppler shift, and represents additive noise, respectively. The Rx then calculates

$$\left(\boldsymbol{z}_{k,\mathrm{p}+}, \boldsymbol{z}_{k,\mathrm{m}}, \boldsymbol{z}_{k,\mathrm{p}-}\right) = \boldsymbol{y}_k\left(\boldsymbol{F}_N^* \otimes \boldsymbol{I}_M\right), \quad (3)$$

where $\boldsymbol{z}_{k,\mathrm{p}+}$, $\boldsymbol{z}_{k,\mathrm{m}}$, $\boldsymbol{z}_{k,\mathrm{p}-}$, and $\boldsymbol{F}^*_N$ are vectors of size $1\times(Q+1)M$, $1\times(2Q+1)M$, $1\times QM$, and the complex conjugate of $\boldsymbol{F}_N$, respectively.

In this case, there is a relationship among $\boldsymbol{p}$, $\boldsymbol{m}$, $\boldsymbol{z}_{k,\mathrm{p}+}$, $\boldsymbol{z}_{k,\mathrm{m}}$, and $\boldsymbol{z}_{k,\mathrm{p}-}$ as

$$\left(\boldsymbol{z}_{k,\mathrm{p}+}, \boldsymbol{z}_{k,\mathrm{p}-}\right) = \boldsymbol{p}\boldsymbol{A}_{k,\mathrm{p}} + \boldsymbol{\eta}_{k,\mathrm{p}}, \quad (4)$$

$$\boldsymbol{z}_{k,\mathrm{m}} = \boldsymbol{m}\boldsymbol{A}_{k,\mathrm{m}} + \boldsymbol{\eta}_{k,\mathrm{m}}, \quad (5)$$

where $\boldsymbol{A}_{k,\mathrm{p}}$ and $\boldsymbol{A}_{k,\mathrm{m}}$ are channel matrices, with elements representing the impulse response between the Tx and Rx and elements of $\boldsymbol{F}_N$. Therefore, the Rx calculates $\boldsymbol{A}_{k,\mathrm{p}}$ by solving Eq. (4) and obtains $\boldsymbol{m}$ by solving

$$\left(\boldsymbol{z}_{1,\mathrm{m}}, \ldots, \boldsymbol{z}_{\beta,\mathrm{m}}\right) = \boldsymbol{m}\left(\boldsymbol{A}_{1,\mathrm{m}}, \ldots, \boldsymbol{A}_{\beta,\mathrm{m}}\right) + \left(\boldsymbol{\eta}_{1,\mathrm{m}}, \ldots, \boldsymbol{\eta}_{\beta,\mathrm{m}}\right). (6)$$

Note that communication quality is expected to improve as the number of β increases and the correlation among $\boldsymbol{A}_{k,\mathrm{m}}$ decreases because the condition number of ($\boldsymbol{A}_{1,\mathrm{m}}$, …, $\boldsymbol{A}_{\beta,\mathrm{m}}$), which represents the noise enhancement factor, decreases. Hence, in the following experiment, we investigate the relationship between communication quality and the intervals δ.

E-mail: [*]ebihara@iit.tsukuba.ac.jp

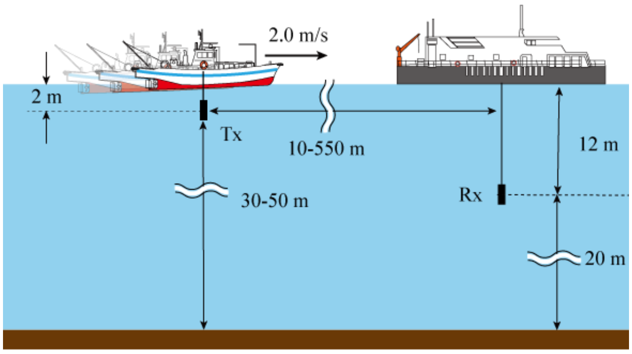

Fig. 2 Experimental environment

3. Experiment and discussions

We performed communication experiments using time-diversity and OSDM in a coastal area of Suruga Bay. **Fig. 2** shows the experimental environment. As shown in the figure, the Tx and Rx were mounted on a boat and a moored barge, respectively. The emitter (OST-2120, OKI seatec) of Tx was set 2 m below the water level, while the hydrophone (BII-7523, Benthowave) of Rx was set 12 m below the water level. During the experiment, the Tx moved at a constant speed of 2 m/s, with the Tx-Rx distance varying from 60 to 523 (m).

Table I summarizes the OSDM parameters used in this experiment. As shown in the table, we investigated five signal patterns (A through E) corresponding to different time intervals. We performed UWA communication by varying the Tx-Rx distance, calculated the output signal-to-noise ratio (OSNR), and analyzed the distribution of OSNR across several Tx-Rx distance regimes.

Figure 3 shows the experimental results indicating the distribution of OSNR for patterns A through E across different Tx-Rx distance regimes [60-150, …, 434-523 (m)], respectively. As shown in these figures, the OSNR improves with increasing interval δ, regardless of the Tx-Rx distance. Furthermore, the improvement in OSNR is more pronounced as the Tx-Rx distance increases, because a larger δ is required to effectively reduce the correlation of $\boldsymbol{A}_{k,\mathrm{m}}$ as the Tx-Rx distance increases.

In summary, it has been found that in UWA communication using time diversity, increasing the retransmission interval improves communication quality. Additionally, the improvement in communication quality is more pronounced, especially when the Tx-Rx distance is large.

4. Conclusion

In this paper, we investigated the relationship between communication quality and signal interval for UWA communication using time-diversity. The experimental results using a mobile platform suggest that the increasing the signal interval is effective, particularly when the Tx-Rx distance is large. Future studies will include investigating the impact on communication quality when varying both β and δ simultaneously.

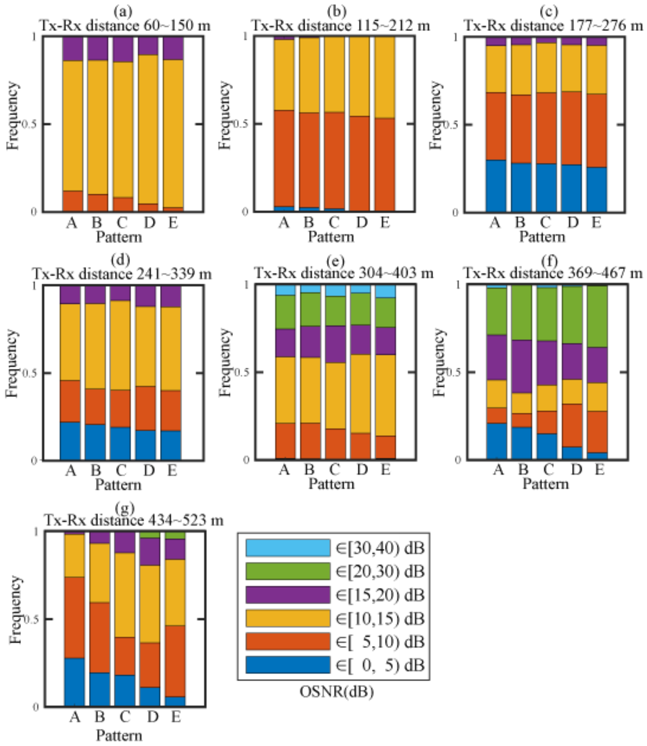

Fig. 3 Experimental results indicating the distribution of OSNR

Table I Parameters used in this experiment

Message length	M	127	
Maximum Doppler shift	Q	2	
Modulation		16QAM	
Signal bandwidth (kHz)		4.8	
Number of signal transmission	β	2	
Signal interval (s)	δ	2	(Pattern A)
		4	(Pattern B)
		6	(Pattern C)
		8	(Pattern D)
		10	(Pattern E)

Acknowledgment

This work was supported by JSPS KAKENHI Grant No. JP 23K26311.

References

1) T. Ebihara, and K. Mizutani, IEEE J. Oceanic Eng. 39, 47 (2014).
2) T. Shimura, Y. Kida, M. Deguchi, Y. Watanabe, and H. Ochi, Jpn. J. Appl. Phys. **54**, 07HG02 (2015)
3) M. Deguchi, Y. Kida and T. Shimura, Jpn. J. Appl. Phys., **58**, SGGF02 (2019).
4) Y. Kida, M. Deguchi, and T. Shimura, Jpn. J. Appl. Phys., **57**, 07LG01 (2019).